Title

COMPARISON OF FINAL STATE APPROXIMATIONS IN THE CALCULATION OF TOTAL AND DIFFERENTIAL PHOTOEMISSION CROSS SECTIONS OF NEON

Author
Williams, R. Stanley

Publication Date
1976-09-01

Submitted to Journal of Chemical Physics

LBL-5413
Preprint C.1

COMPARISON OF FINAL STATE APPROXIMATIONS IN THE CALCULATION OF TOTAL AND DIFFERENTIAL PHOTOEMISSION CROSS SECTIONS OF NEON

R. Stanley Williams and D. A. Shirley

September 1976

Prepared for the U. S. Energy Research and Development Administration under Contract W-7405-ENG-48

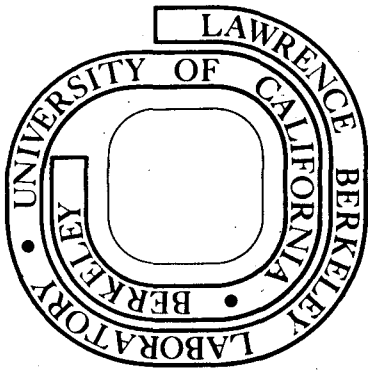

DISCLAIMER

COMPARISON OF FINAL STATE APPROXIMATIONS IN THE CALCULATION OF TOTAL AND DIFFERENTIAL PHOTOEMISSION CROSS SECTIONS OF NEON *

R. Stanley Williams and D. A. Shirley

Materials and Molecular Research Division
Lawrence Berkeley Laboratory
and
Department of Chemistry
University of California
Berkeley, California 94720

ABSTRACT

Differential photoemission cross sections for the 1s, 2s, and 2p shells of neon were calculated by several different approximations for photon energies up to 2000 eV. Specifically, plane-wave (PW), orthogonalized plane wave (OPW), and Hartree-Fock functions (with and without consideration of relaxation in the final ionic state) were used to compute transition matrix elements in both velocity and length approximations. Plane wave and orthogonalized plane wave continuum functions were found to have very limited applicability to cross section calculations, with both approximations giving spurious local minima and incorrect angular distributions. The reasons for these failures were analyzed, and limits were set on the n, ℓ, and Z values for which the PW model yields qualitatively correct total cross sections. Calculations using Hartree Fock continuum functions agree very well with experiment, emphasizing the necessity of considering atomic potentials explicitly in photoemission processes. Further, the effects of relaxation in the final bound system were investigated. They were small for valence electrons and only slightly more important for Ne 1s core electrons. Applications of these findings to photoemission from molecules and absorbates are discussed briefly.

INTRODUCTION

Observation of photoemission spectra provides detailed information about both the initial and final electronic structure of the system under study. Energy and angular dependent studies of photoemission cross sections made possible by several new photon sources, especially synchrotron radiation, can provide a sensitive probe of gaseous species, liquids, solid surfaces, and adsorbates. However, in order to interpret PES in terms of electronic structure a good model of the transition from initial to final states is necessary.

The detailed many-electron theory of photoemission for gaseous atomic species is well known.[1] Recently, steps have been taken to formulate viable theories of photoemission for molecular species[2] and solid surfaces.[3] In many cases, these approaches consider one-electron transitions to final continuum states that are approximated by a plane wave (PW) or an orthogonalized plane wave (OPW).[4] The validity of calculations employing PW or OPW continuum functions and neglecting final state relaxation must be established before they may be applied to the interpretation of experimental results that are now appearing.

In this paper, we report photoemission cross sections and asymmetry parameters[5] for the 1s, 2s and 2p orbitals of neon, calculated by several methods. Intercomparisons of these results and comparison with experiment are utilized to ascertain the validity of the various approximations employed. In Section II we focus on various approximations to the continuum functions, and Section III deals with the effects of final state relaxation. Further discussion is given in Section IV.

CONTINUUM WAVEFUNCTIONS

The final state of a photoemission transition is of special interest because at least one electron of the system under study is in the continuum. In this section we compare the differential photoemission cross section $d\sigma(\varepsilon)/d\Omega$ of neon, calculated using plane wave (PW), orthogonalized plane wave (OPW), and Hartree-Fock (HF), continuum functions, with experiment. We test the sensitivity of photoemission cross sections to the form of the final state continuum function to evaluate the accuracy of the PW and OPW approaches. We shall find that calculated neon cross sections depend strongly on the model used for the continuum state and that both the PW and OPW models are quite poor approximations for those continuum states which exhibit large phase shifts.

Following Cooper and Manson,[6] we write the differential photoemission cross section from the $n\ell^{th}$ shell of an atom as a function of final state continuum electron kinetic energy ε in the dipole approximation as

$$\frac{d\sigma_{n\ell}(\varepsilon)}{d\Omega} = \frac{\sigma_{n\ell}(\varepsilon)}{4\pi}\left[1 - \frac{1}{2}\beta(\varepsilon)\ P_2(\cos\theta)\right] \quad , \tag{1}$$

where Θ is the angle between an incident beam of unpolarized radiation and the photoelectron wave vector. In the one electron partial wave approximation the total cross section is

$$\sigma_{n\ell}(\varepsilon) = \frac{\omega(2\pi)^2 e^2 \hbar^2}{c}\ \frac{N_{n\ell}}{3(2\ell+1)}\left[\ell\left(R^{\varepsilon\ell-1}_{n\ell}\right)^2 + (\ell+1)\left(R^{\varepsilon\ell+1}_{n\ell}\right)^2\right] \tag{2}$$

where ω is the angular frequency of the incident radiation, $N_{n\ell}$ is the occupation number of the $n\ell^{th}$ subshell, and the $R_{n\ell}^{\varepsilon\ell\pm1}$ are defined in the dipole length and velocity formulations by

$$R_{n\ell}^{\varepsilon\ell\pm1} = \int_0^\infty P_{\varepsilon\ell\pm1}(r)\ rP_{n\ell}(r)\ dr = \tag{3}$$

$$\frac{1}{M_e\omega}\int_0^\infty P_{\varepsilon\ell\pm1}(r)\left(\frac{d}{dr} + \frac{2\ell+1\pm1}{2r}\right) P_{n\ell}(r)\ dr \quad .$$

The continuum functions $P_{\varepsilon\ell}(r)$ are normalized to a Dirac delta function in ε.[7]

The asymmetry parameter[8] $\beta(\varepsilon)$ is given by

$$\beta(\varepsilon) = \tag{4}$$

$$\frac{\ell(\ell-1)\left(R_{n\ell}^{\varepsilon\ell-1}\right)^2 + (\ell+1)(\ell+2)\left(R_{n\ell}^{\varepsilon\ell+1}\right)^2 - 6\ell(\ell+1)\left(R_{n\ell}^{\varepsilon\ell-1}\right)\left(R_{n\ell}^{\varepsilon\ell+1}\right)\cos\left(\xi_{\ell+1}-\xi_{\ell-1}\right)}{(2\ell+1)\left[\ell\left(R_{n\ell}^{\varepsilon\ell-1}\right)^2 + (\ell+1)\left(R_{n\ell}^{\varepsilon\ell+1}\right)^2\right]}$$

for continuum function phase shifts $\xi_{\ell\pm1}(\varepsilon)$ in the $\ell \pm 1$ channel defined for scattering from a nonzero potential.

In this formulation we explicitly consider two outgoing channels for the photoemitted electron defined by dipole selection rules. The total photoelectron flux depends only upon the sum of the electron fluxes in the two channels, but the angular dependence of intensity is sensitive to the interference between the channels. Thus the phase shifts $\xi_{\ell\pm1}(\varepsilon)$ can have a significant effect upon the angular distribution of photoelectron flux.

Utilizing the Rayleigh expansion[9] of a plane wave we see that the PW state contains contributions from all integral values of angular

momentum. The normalized radial component of the PW ℓ channel is

$$P^{PW}_{\varepsilon\ell}(r) = \sqrt{\frac{2M_e k}{\pi\hbar^2}} r j_\ell(kr) \tag{5}$$

$$\xrightarrow{r \to \infty} \sqrt{\frac{2M_e}{\pi\hbar^2 k}} \sin\left(kr - \frac{1}{2}\ell\pi\right) \quad .$$

where $j_\ell(kr)$ is a Spherical Bessel Function. In this zeroth order Born approximation the interaction of the continuum electron with the remaining atomic charges is completely ignored. One way to introduce an effective atomic potential[10] is to Schmidt orthogonalize the continuum channels to the bound states of the system. The radial component of the OPW is then

$$P^{OPW}_{\varepsilon\ell} = \sqrt{\frac{2M_e k}{\pi\hbar^2}} \left\{ r j_\ell(kr) - \sum_{\ell'=\ell} \int_0^\infty P_{n'\ell'}(r)\, r j_\ell(kr)\, dr P_{n'\ell'}(r) \right\} \tag{6}$$

where the summation is taken over all bound states with the same angular momentum quantum number as the continuum channel. This orthogonalization alters the wavefunction near the origin but has no effect on its delta function normalization or asymptotic form (i.e., no phase shift is introduced).

A more exact method of treating the continuum function is to require that it be the eigenfunction of an atomic Hamiltonian. In our study we integrated the single particle Hartree-Fock equation numerically for the given atomic configuration[11] and continuum electron kinetic energy ε. The asymptotic form of these numerical solutions is

$$P^{HF}_{\varepsilon\ell}(r) \xrightarrow[r\to\infty]{} \sqrt{\frac{2M_e}{\pi\hbar^2 k}} \sin\left(kr - \frac{1}{2}\ell\pi - \frac{e^2 M_e}{\hbar^2 k}\ln 2kr + \xi_\ell(\varepsilon)\right) \quad , \tag{7}$$

where

$$\xi_\ell(\varepsilon) = \delta_\ell(\varepsilon) + \sigma_\ell(\varepsilon) \quad , \tag{8}$$

$$\sigma_\ell(\varepsilon) = \arg\Gamma\left(\ell + 1 - i\frac{e^2 M_e}{\hbar^2 k}\right) \tag{9}$$

and $\delta_\ell(\varepsilon)$ is the phase shift of the HF continuum function with respect to the regular Coulomb wavefunction. The wavefunctions were generated using Bates' program[12] modified to yield phase shifts.[13] The bound state orbitals used were those of Bagus.[14]

We used the partial wave approach for the PW and OPW cross section calculations to allow a direct comparison with our more exact HF results. Another mathematically equivalent formation utilizes the fact that a plane wave is an eigenfunction of the momentum operator.[15] The dipole velocity transition matrix element is proportional to the product of the magnitude of the electron wave vector and the Fourier transform of the initial-state orbital. Including the constraint of orthogonality to the bound state orbitals yields the total cross section

$$\sigma_T(\varepsilon) = \frac{8\pi e^2 k}{3M_e c\omega} \frac{N_{n\ell}}{(2\ell+1)} \Big\{(2\ell+1)\, k^2 f^2_{n\ell} + \ell\left(G^2_{\ell-1} + 2kf_{n\ell}G_{\ell-1}\right) + (\ell+1)\left(G^2_{\ell+1} - 2kf_{n\ell}G_{\ell+1}\right)\Big\} \tag{10}$$

and the asymmetry parameter

$$\beta(\varepsilon) = \Big[2(2\ell+1)^2 k^2 f_{n\ell}^2 + \ell(\ell-1)\left(G_{\ell-1}^2 + 2kf_{n\ell}G_{\ell-1}\right) + (\ell+1)(\ell+2)$$

$$\left(G_{\ell+1}^2 - 2kf_{n\ell}G_{\ell+1}\right) + 6\ell(\ell+1)(kf_{n\ell}G_{\ell-1} - kf_{n\ell}G_{\ell+1} - G_{\ell-1}G_{\ell+1})\Big] / \quad (11)$$

$$\Big\{(2\ell+1)\Big[(2\ell+1)\,k^2 f_{n\ell}^2 + \ell\left(G_{\ell-1}^2 + 2kf_{n\ell}G_{\ell-1}\right) + (\ell+1)\left(G_{\ell+1}^2 - 2kf_{n\ell}G_{\ell+1}\right)\Big]\Big\},$$

where

$$f_{n\ell} = \int^{\infty} rj_{\ell}(kr)\; P_{n\ell}(r)\; dr \quad (12)$$

and

$$G_{\ell\pm1} = \sum_{n'} \int_0^{\infty} rj_{\ell\pm1}(kr)\; P_{n'\ell\pm1}(r)\; dr \int_0^{\infty} P_{n'\ell\pm1}(r) \quad (13)$$

$$\left(\frac{d}{dr} + \frac{2\ell+1\pm1}{2r}\right)\; P_{n\ell}(r)\; dr \quad ,$$

for photoemission from the $n\ell^{th}$ one-electron orbital and the summation extending over the bound orbitals with the same symmetry as the $\ell \pm 1$ continuum channel.

From Eq. (11) we see that $\beta(\varepsilon) = 2$ for plane wave photoionization independent of the energy ε and the symmetry of the initial bound state. In the OPW case, β can assume values other than 2, but must approach 2 in the limit of large k. The remaining discussion of PW and OPW cross sections will deal with the partial-wave form. In these cases, the velocity and length total cross sections have the same qualitative appearance, but the length calculations yield cross sections an order of magnitude greater than the velocity results. The PW and OPW length results are excluded from the following discussion.

Comparisons of $\sigma_{n\ell}(\varepsilon)$ and $\beta_{2p}(\varepsilon)$ calculated for the various continuum wavefunction approximations with experiment are shown in Figs. 1-4. The PW and OPW calculations give poor results for 1s and 2s photoemission, but the 2p total cross section results are qualitatively correct. However, the angular dependence given by the PW and OPW calculations for 2p photoemission is totally incorrect. The different HF continuum function calculations agree very well with experiment, and will be more thoroughly discussed in the next section. In the remainder of this section we discuss the PW and OPW results.

For 1s photoemission (Fig. 1), the PW velocity cross section rises slowly by several orders of magnitude from threshhold to a maximum near a photon energy of 1400 eV and then falls gradually at higher energies. The OPW calculation is closer to the observed cross section at threshhold, but then falls to a spurious local minimum at about 1050 eV and rises from there to approach the PW cross section asymptotically. The PW and OPW results are qualitatively incorrect for $h\nu < 1500$ eV and have not attained the correct slope at $h\nu = 2000$ eV. Orthogonalization of the plane wave for the $1s \rightarrow \varepsilon p$ photoemission channel does not improve the calculated cross section over the PW case.

The $2s \rightarrow \varepsilon p$ channel (Fig. 2) shows large increases in cross section at threshhold and spurious minima for both PW and OPW calculations. Again the slope at high photon energy is too gradual and the OPW result is no better than the PW result.

The $2p \rightarrow (\varepsilon s, \varepsilon d)$ PW and OPW calculations (Fig. 3) are quite close to both the HF and experimental results. The PW and OPW values are too large at higher energies, but they appear to have the correct

limiting slope. Orthogonalization of the εs channel to the 1s and 2s occupied orbitals appears to have improved the agreement with experiment considerably in the medium energy range. Finally, both PW and OPW cross sections are fair even close to threshhold.

The $\beta_{2p}(\varepsilon)$ values for the PW and OPW partial wave calculations are in serious disagreement with both HF and experimental results, as shown in Fig. 4. The PW $\beta_{2p}(\varepsilon)$ value calculated by Eq. (4) is 2, as predicted by Eq. (11). The OPW $\beta_{2p}(\varepsilon)$ results are not correct, either. Thus, although OPW and PW closely predict the 2p total cross section, they fail badly in describing the differential cross section.

We interpret these findings in terms of the behavior of the continuum functions in the region of space where the bound atomic states have appreciable amplitude, and correlate this behavior with the phase shifts of the "actual" continuum functions. An illustration of this effect is offered in Fig. 5. Here we see the radial parts of the HF and PW continuum functions for 1s photoionization at $h\nu$ = 1100 eV, near the region where OPW theory predicts a spurious minimum in the cross section. Although the shape of the two continuum functions is virtually identical after the first period there is a significant positive phase shift of the HF continuum function with respect to the plane wave. This phase shift reflects the different behavior of the two wavefunctions near the nucleus. It can be seen that the HF continuum function is orthogonal to the 2p radial wavefunction (the overlap integral is less than 10^{-5}). It is also fairly obvious that orthogonalizing the plane wave to the 2p wavefunction will decrease the PW amplitude in the radial region where the 1s radial function is

large, thus resulting in a very small transition matrix element. This result is independent of the relative phases of the wavefunctions involved. An analytical illustration of this result is obtained by writing Eq. (6) in the simple form

$$|\text{OPW}\rangle = |\text{PW}\rangle - \langle 2p|\text{PW}\rangle|2p\rangle \quad , \tag{14}$$

then calculating $\langle 1s|\vec{\nabla}|\text{OPW}\rangle$, which will be minimal in the energy range for which

$$\langle 1s|\vec{\nabla}|\text{PW}\rangle \triangleq \langle 1s|\vec{\nabla}|2p\rangle\langle 2p|\text{PW}\rangle \quad . \tag{15}$$

Now $\langle 1s|\vec{\nabla}|2p\rangle$ is a constant, while $\langle 1s|\vec{\nabla}|\text{PW}\rangle$ and $\langle 2p|\text{PW}\rangle$ are proportional to Fourier transforms of the $|1s\rangle$ and $|2p\rangle$ atomic functions. Since both $|1s\rangle$ and $|2p\rangle$ are nodeless, the Fourier transform of each will rise with increasing energy to maxima, then decrease, with the maximum for the $|2p\rangle$ Fourier transform coming at a lower energy than that of the $|1s\rangle$. Since the value of $\langle 1s|\vec{\nabla}|2p\rangle$ is in general large, a cross over energy will exist at which $\langle 1s|\vec{\nabla}|\text{OPW}\rangle = 0$. This spurious zero in σ_{1s} is an inevitable and completely artifical consequence of attempting to represent the continuum state by a basis set of only the two functions $|\text{PW}\rangle$ and $|2p\rangle$.

Examination of Fig. 6 shows the phase shifts $\delta_\ell(\varepsilon)$ of the HF continuum functions. The phase shifts $\sigma_\ell(\varepsilon)$ are much smaller than $\delta_\ell(\varepsilon)$ for all but the lowest energies. The εs and εp photoemission channels have large phase shifts with respect to normal Coulomb waves. Thus, for these channels, both Coulomb waves and plane waves ($V(r) = \frac{1}{r}$ and $V(r) = 0$ continuum functions) must differ greatly from the actual continuum functions for small r. Matrix elements calculated with these approximations will be very much in error. However, the εd channel phase shifts are fairly small and the $\ell = 2$ part of a plane wave

should be a good approximation to the HF and "actual" continuum functions. Comparison of the individual matrix elements for $s \rightarrow p$, $p \rightarrow s$, and $p \rightarrow d$ transitions confirms these expectations (Table 1).

The fair agreement with experiment of the PW and OPW total cross section calculations results from the dominance of the εd channel to the total photoemission cross section. The improvement of the OPW results over the PW results is due to a fortuitous cancellation of εS intensity by the orthogonalization to 1s and 2s states. Since the HF 2p cross section is ~90% d-channel contribution over most of the energy range of Fig. 3, we see that the PW approximation is improved by considering only the $2p \rightarrow \varepsilon d$ PW channel. The marked disagreement between experimental and OPW asymmetry parameters arises because of the poor OPW εs channel approximation and the absence of phase shift information.

We now wish to establish the limits within which OPW and PW calculations may be used at least semi-quantitatively. Consulting Manson's paper[16] on the Z, ℓ, and ε dependence of continuum electron phase shifts calculated in a central-potential model, we note the excellent agreement between the phase shifts of Fig. 6 and those calculated by Manson for $Z = 10$. By considering continuum channels with small phase shifts, we can assign rough upper limits on the Z for which plane waves should be fair approximations to the "actual" continuum functions. We find that only final states of transitions $\ell \rightarrow \ell + 1$ are well approximated by plane waves. For a particular angular momentum ℓ continuum function phase shifts become large for Z just great enough to have a bound state with angular momentum ℓ. Thus

there is no real justification for prefering OPW's over PW's for any case. Calculations for which only the $\ell \rightarrow \ell + 1$ PW channel is considered should yield fair total photoemission cross sections for 1s and 2s shells up to Z = 4, 2p shells up to Z = 12, 3d shells up to Z = 38, and 4f shells up to Z = 88. For slightly higher atomic numbers results should be qualitatively correct, but agreement cannot be expected when Z is almost large enough to support a bound shell with the same symmetry as the continuum channel in question. For initial states with a node in the radial wavefunction, a PW cross section calculation will yield a marked local minimum in the cross section as a function of energy (Fig. 2 and Ref. 17), but assignment of this minimum as a spurious result or a real Cooper minimum requires care. Finally, it should be emphasized that the angular dependence for a PW approximation can only be correct for photoemission from an atomic s orbital.

III. FURTHER FINAL STATE CONSIDERATIONS

Previous exhaustive and extensive studies of atomic photoemission processes[5] have explicitly considered the effects of intrachannel coupling, core relaxation, interchannel coupling, and electron correlation. In our calculations, only single-configuration initial and final states were utilized. Intrachannel coupling was treated implicitly through the use of the Hartree-Fock continuum functions[18] for cases both with and without inclusion of core relaxation. Interchannel coupling was neglected, but has already been shown to be small for neon photoemission.[19]

The inclusion of final-state relaxation in the transition model modifies the HF results in three ways. First, the one-electron transition matrix element is changed because the continuum wavefunction is calculated in the relaxed potential of the ion. Second, because one-electron orbitals of the initial and final states with the same symmetry but different principal quantum numbers are no longer orthogonal, virtual transitions of the type ($1s \rightarrow 2p$, $2p \rightarrow \varepsilon p$) are now allowed. Finally, because equivalent passive orbitals of the initial and final states are not identical, their overlap integrals must be less than unity, which will decrease all the contributions to the total matrix element. The expressions for the total cross section, Eq. (2), and the asymmetry parameter, Eq. (4) retain the same form in the case of excitations from closed shells except that the one-electron radial matrix elements for a transition from a one-electron initial state $n\ell$ to a final continuum state $\varepsilon\ell\pm1$ are replaced by sums over radial matrix elements of the form

$$IR_{n\ell}^{\varepsilon\ell\pm1} = \sum_{k=1}^{N} \det \left\{ \int_0^\infty P'_{\tau(i)}(r)\ \hat{O}_j^k\ P_{\tau(j)}(r)\, dr \right\} , \tag{14}$$

$$\hat{O}_j^k = \begin{cases} 1 \text{ for } j \neq k \\ r \text{ or } \frac{1}{M_e \omega} \left(\frac{d}{dr} + \frac{2\ell_j + 1 \pm 1}{2r} \right) \text{ for } j = k \end{cases} , \tag{15}$$

where N is the total number of electrons of the system and the curly brackets denote an N × N matrix with column index i ($\tau(i) = (n\ell m_\ell m_s)_i$) for the N different final state one-electron orbitals, including the continuum orbital, and row index j, for the N initial state orbitals. The final state radial wavefunctions are primed to emphasize that they are not identical to the corresponding initial state orbitals. The ij^{th} element is zero for $j \neq k$ unless $(\ell m_\ell m_s)_i = (\ell m_\ell m_s)_j$ and is zero for $j = k$ unless $(\ell m_\ell m_s)_i = (\ell \pm 1\ m_\ell m_s)_j$. Thus the transition matrix element for the HFR (HF with relaxation) case may be quite different from the corresponding one-electron HF matrix element.

The neon 1s photoemission cross sections for the length and velocity approximations differed by less than 1% in both the HF and HFR calculations. At energies above 1200 eV the HFR cross sections agree quite well with experiment (Fig. 2), and are to be preferred over the HF results. However, at lower energies the HF calculation is closer to experiment except at threshhold (Fig. 1, insert). This is probably due to the neglect of correlation between the slow photoelectron and the electrons of the remaining ion in our calculations. Right at threshhold the virtual processes are quite important, but at higher energies they become small (see Fig. 7). The turning-over of the experimental σ(1s) as threshhold is approached from above (Fig. 1, insert) arises from such processes, and it is significant

that the HFR model reproduces this behavior while HF does not. The phase shifts for the HF and HFR εp continuum functions (Fig. 6) differ by 10% over the whole range of the calculation, showing the fairly large effect of the relaxed potential in determining the continuum wavefunction for an electron excited from a core state.

Relaxation effects are small for neon 2s photoemission, as seen by the small differences in continuum function phase shifts (Fig. 6) and total cross sections (Fig. 2). The HF and HFR cross-section calculations are only distinguishable below 200 eV photon energy, where the HFR velocity approximation is seen to agree most closely with experiment.

Relaxation changes the potential experienced by the photoelectron very little for the 2p photoemission, yet the εd channel phase shifts (Fig. 6) differ significantly for HF and HFR continuum functions at low energy. However, the cross section and asymmetry parameter differences are very small for the two approaches (Figs. 3 and 4). Both the energy and angular dependence of 2p photoemission calculations are in excellent agreement with experiment, with the velocity results being slightly superior.

Slight oscillations[20] occur in the calculated HF and HFR asymmetry parameters above 500 eV which are absent from the OPW calculations. However, these oscillations, which amount to 2% or less of the magnitude of β, are not entirely consistent among the various HF calculations. Further calculations of β utilizing CI wavefunctions for the initial and final states--and small energy separations between values of β(ε) are required to evaluate whether these oscillations are

indeed real or artifacts of the present calculation.

For the cases reported here virtual excitation processes were largely compensated by the change in the one-electron matrix elements due to the relaxed potential. Relaxation is seen to have a very small effect on valence orbital photoemission at all but the lowest photon energies.

IV. DISCUSSION

We now discuss the work of other authors in terms of our results.

Rabalais and co-workers[21] calculated photoemission cross sections for neon and several small molecules using PW and OPW continuum functions. They reported results for Ne PW total cross sections that agree closely with our PW results, but they did not list enough OPW cross sections to make comparisons. Molecular photoemission total cross sections calculated by the PW approach for CH_4, NH_3, and H_2O resemble the Ne results closely[21] and can be only slightly better due to the smaller nuclear charges of the central species (we note specifically that all these molecular calculations exhibit a local minimum in 2s-like shells similar to that in Fig. 2). Calculations for s-like shells of molecules with more massive atoms, such as H_2S are probably not qualitatively correct. One major difference we note between our calculations and the OPW results of Rabalais et al. is for the asymmetry parameter in Ne 2p photoemission at 1254 eV photon energy. Rabalais et al. reported a value of 0.719, where we observe that the OPW β is 1.55 and is slowly approaching the PW asymptotic value of 2.

Other workers have also considered molecular photoionization. Hush[22] used a model in which the average potential experienced by the photoelectron is used to give an effective kinetic energy for the continuum electron. This model yields slightly improved total cross sections for small molecules, but will still have the same difficulties as the PW method for large atoms and will be unable to yield angular distributions of photoelectrons. Ritchie[23] and Chapman[24] are currently

developing procedures to calculate molecular photoemission which explicitly consider the nuclear and electronic Coulomb potentials. Pseudopotential models have also been considered,[25] but depend on some auxiliary method of determining the phase shifts for the continuum channels. There are also strong interchannel coupling effects[26] at low energies which are strictly molecular phenomenon that require accurate wavefunctions to handle properly. We discourage reliance on PW type calculations and stress the need to consider the strong forces acting on continuum electrons in calculating photoionization and photodetatchment cross sections for atoms and molecules.

Gadzuk and Liebsch[4] have considered photoemission from adsorbates on oriented surfaces in PW approximations. Their work has concentrated on obtaining angular distributions of photoelectrons from the adsorbate-surface system. Although the angular dependence of photoemission for a given ℓ channel of an adsorbed species and surface geometry may be correctly determined, the plane wave treatment is incapable of treating interference between different allowed ℓ channels. Even in spectral regions where the total cross section is dominated by one particular channel the angular dependence of the photoemitted electron current may be strongly influenced by the less intense channel (witness Ne 2p photoemission). Thus, the necessity of including some potential model for photoemission from surfaces must be emphasized. To our knowledge, no calculations of this type have yet appeared in the literature.

Finally, we note that due to the present state of the theory of photoemission from gases and adsorbed species, inclusion of relaxation

effects in cross section calculations is unnecessary. We have seen that for valence-shell photoemission these effects are noticeable only near threshhold. However, in these low energy regions resonance effects in molecules and plasma interactions on surfaces would also have to be included to make the relaxation effects meaningful.

ACKNOWLEDGEMENT

The authors wish to express their gratitude to Dr. Richard L. Martin for suggesting the topics included in this paper and for many helpful discussions during the course of this investigation.

FOOTNOTES AND REFERENCES

*This work was done with support from the U.S. Energy Research and Development Administration.

1. U. Fano and J. W. Cooper, Rev. Mod. Phys. 40, 441 (1968); J. Cooper and R. N. Zare, Lectures in Theoretical Physics, Vol. 11c, edited by S. Geltman, K. Mahanthappa, and W. Brittin (Gordon and Breach, New York, 1969), pp. 317-337.

2. B. Ritchie, J. Chem. Phys. 60, 898 (1974); B. Schneider and R. S. Berry, Phys. Rev. 182, 141 (1969).

3. B. Feuerbacher and R. F. Willis, J. Phys. C 9, 169 (1976); G. D. Mahan, Phys. Rev. B 2, 4334 (1970).

4. F. O. Ellison, J. Chem. Phys. 61, 507 (1974); J. W. Gadzuk, Phys. Rev. B 12, 5030 (1974); A. Liebsch, Phys. Rev. B 13, 544 (1976).

5. Ne differential photoemission cross sections have been calculated by many authors using different approaches. R. J. W. Henry and L. Lipskey, Phys. Rev. 153, 51 (1967); M. Y. Amusia, N. A. Cherepkov, and L. V. Chernysheva, (Sov. Phys.-JETP 33, 90 (1971); D. J. Kennedy and S. T. Manson, Phys. Rev. A 5, 227 (1972); F. M. Chapman and L. L. Lohr, Jr., J. Amer. Chem. Soc. 96, 4731 (1974); P. G. Burke and K. T. Taylor, J. Phys. B 8, 2620 (1975); R. L. Martin and D. A. Shirley, Phys. Rev. A 13, 1475 (1976).

6. J. W. Cooper and S. T. Manson, Phys. Rev. 177, 157 (1969).

7. R. A. Buckingham, Quantum Theory I. Elements, edited by D. R. Bates (Academic Press, New York, 1961), p. 147.

8. See especially the second reference of footnote 1.

9. A. R. Edmonds, Angular Momentum in Quantum Mechanics, (Princeton University Press, Princeton, 1960), p. 80.

10. L. L. Lohr, Jr., Electron Spectroscopy, edited by D. A. Shirley, (North-Holland, Amsterdam, 1972), p. 245.

11. For further discussion see the third reference of footnote 5.

12. G. N. Bates, Computer Phys. Commun. 8, 220 (1974).

13. M. J. Seaton and G. Peach, Proc. Phys. Soc. (London) 79, 1296 (1962).

14. P. S. Bagus, Phys. Rev. 139, A619 (1965).

15. H. A. Bethe and E. E. Salpeter, Quantum Mechanics of One- and Two-Electron Atoms, (Springer-Verlag, Berlin, 1957), pp. 295-320.

16. S. T. Manson, Phys. Rev. 182, 97 (1969).

17. P. S. Wehner, J. Stöhr, G. Apai, F. R. McFeely, R. S. Williams, and D. A. Shirley, submitted to Phys. Rev. B.

18. See section 5 of the first reference of footnote 1.

19. See the first reference of footnote 5.

20. Oscillations of this type in calculations of β have also been observed by C. Fadley (private communication).

21. J. W. Rabalais, T. P. Debies, J. L. Berkosky, J.-T. J. Huang, and F. O. Ellison, J. Chem. Phys. 61, 516 (1974); J. W. Rabalais, T. P. Debies, J. L. Berkosky, J.-T. J. Huang, and F. O. Ellison, J. Chem. Phys. 61, 529 (1974); J. W. Rabalais and T. P. Debies, J. Electron Spectrosc. 5, 847 (1974).

22. P. R. Hilton, S. Nordholm, and N. S. Hush, to be published.

23. B. Ritchie, J. Chem. Phys. 60, 898 (1974); B. Ritchie, J. Chem. Phys. 61, 3279 (1974); B. Ritchie, J. Chem. Phys. 63, 1351 (1975).

24. F. M. Chapman, private communication.

25. B. Schneider and R. S. Berry, Phys. Rev. 182, 141 (1969).

26. J. L. Dehmer and D. Dill, to be published.

27. F. Wuilleumier, Adv. X-ray Anal. 16, 63 (1973).

28. J. A. R. Samson, J. Opt. Soc. Am. 55, 8, 935 (1965).

Table I.[a]

Photon Energy	2s → εp		2p → εs		2p → εd	
	HF	PW	HF	PW	HF	PW
50	.205	-.074	-.199	.441	-.445	-.342
100	.332	-.447	-.154	.484	-.437	-.375
200	.329	-.121	-.110	.388	-.307	-.301
300	.293	-.036	-.086	.309	-.216	-.239
400	.260	-.110	-.070	.251	-.161	-.195
500	.233	-.147	-.059	.210	-.126	-.162
1000	.153	-.171	-.031	.105	-.055	-.081
1500	.114	-.147	-.020	.065	-.044	-.050
2000	.091	-.125	-.014	.045	-.022	-.035

[a] Numerical values of the matrix element $< f|\frac{d}{dz}|i >$ for initial states (i) 2s and 2p and for some HF and PW final states (f). Note that the plane wave matrix elements for the 2s → εp and 2p → εs transitions have the opposite sign of the corresponding HF matrix elements.

FIGURE CAPTIONS

Fig. 1. Calculated neon 1s photoionization cross sections versus photon energy compared with the experimental values of Wuilleumier (W) in ref. 27. For the Hartree-Fock continuum function calculations the dipole length and velocity approximations yield results indistinguishable on the scale presented here.

Fig. 2. Calculated neon 2s photoionization cross sections versus photon energy. The experimental values (W) are from ref. 27. Dipole length and velocity approximations are denoted by L and V respectively.

Fig. 3. Calculated neon 2p photoionization cross sections versus photon energy. The experimental values are (W) from ref. 27 and (S) from ref. 28.

Fig. 4. The asymmetry parameter β for neon 2p photoionization as a function of photon energy. The experimental values (W) are from ref. 27.

Fig. 5. Comparison of the radial part of the HF εp wave ejected from Ne 1s by an 1100 eV photon with the p component of a plane wave with identical kinetic energy. The continuum functions in this figure are not normalized.

Fig. 6. The phase shift $\delta(\varepsilon,\ell)$ with respect to a normal Coulomb wave for Hartree-Fock continuum functions calculated in unrelaxed and relaxed (R) final state atomic potentials versus continuum electron kinetic energy.

Fig. 7. Percent contribution to the total n electron transition matrix element due to the various virtual processes allowed when relaxation is considered in the Ne 1s photoionization.

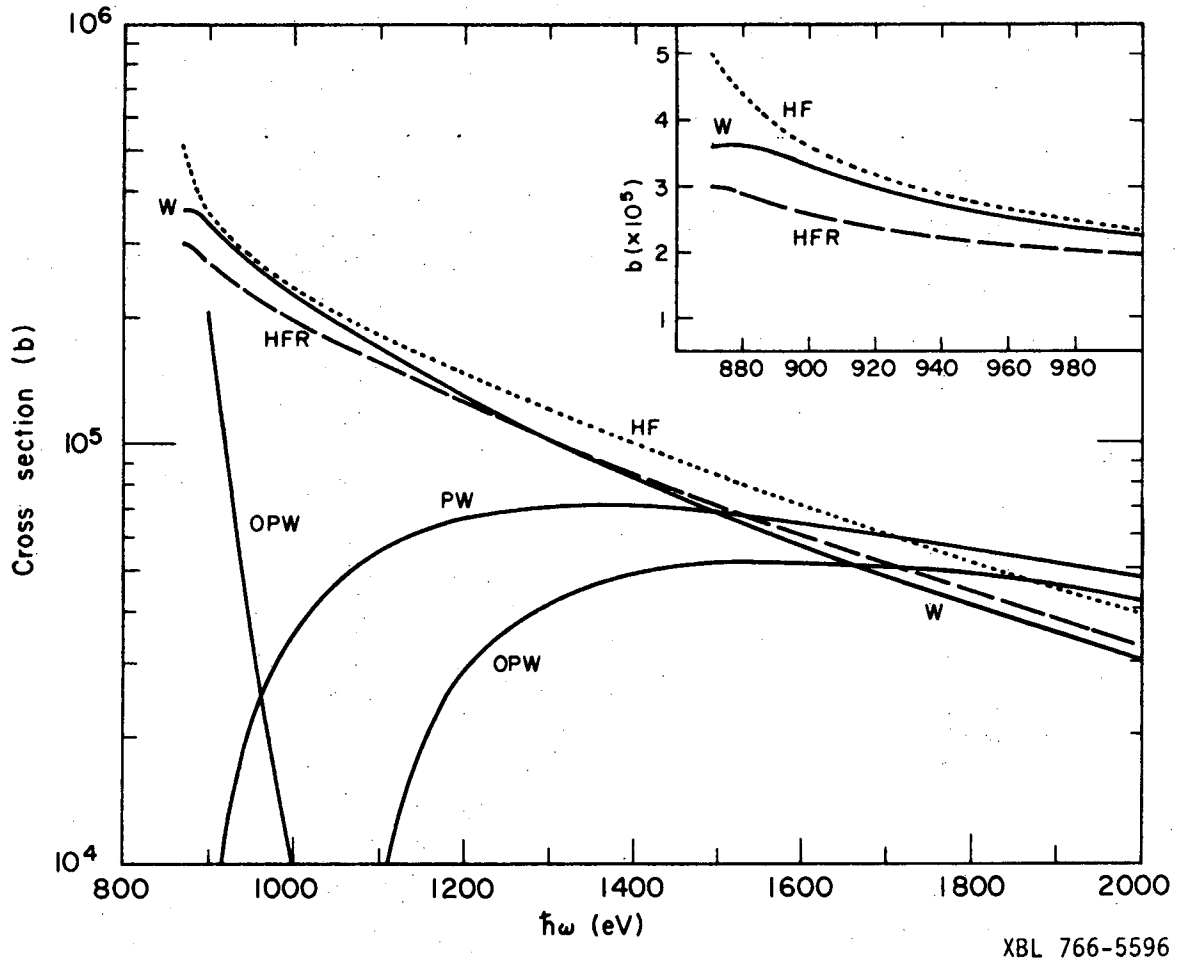

XBL 766-5596

Fig. 1

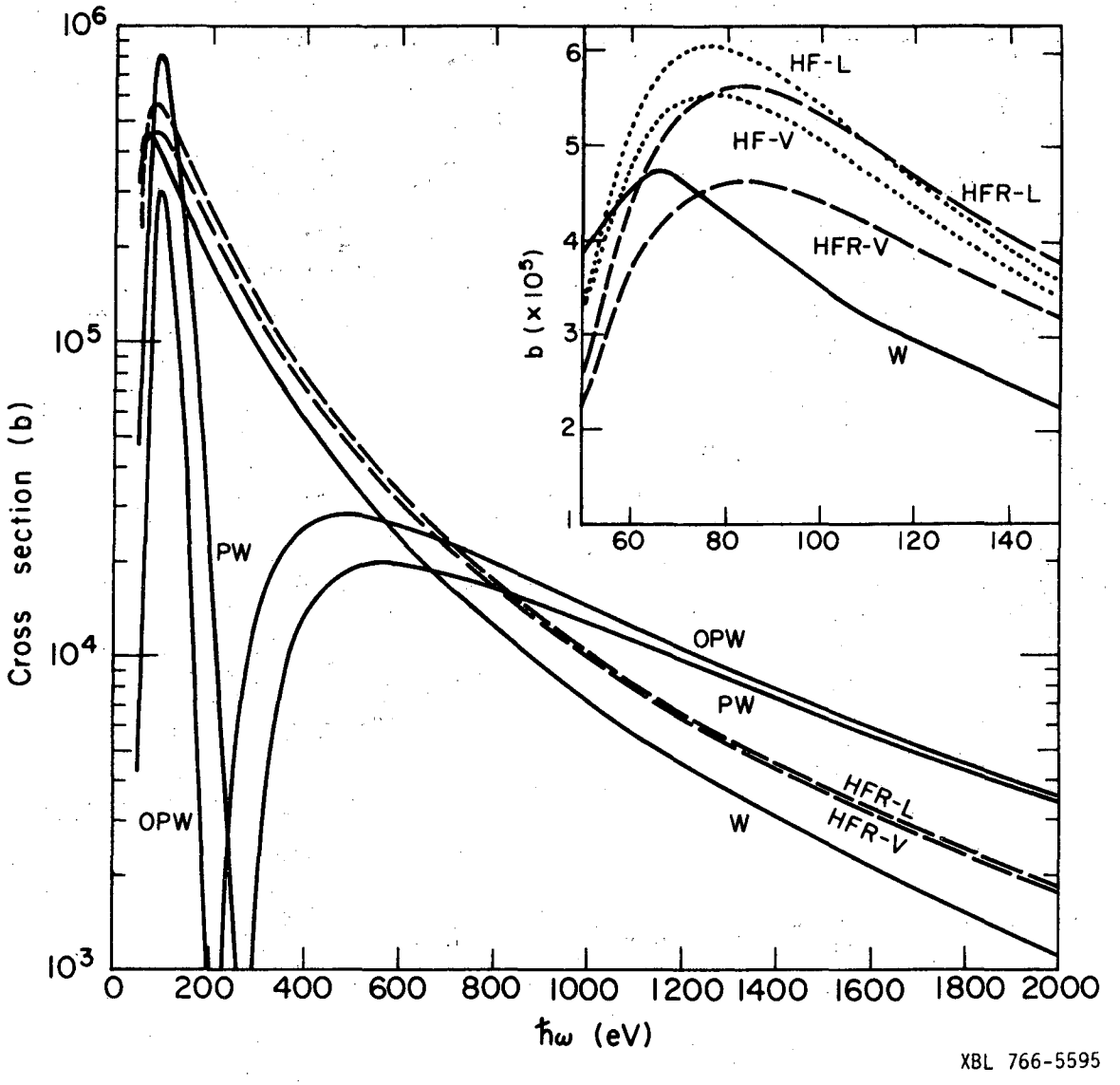

Fig. 2

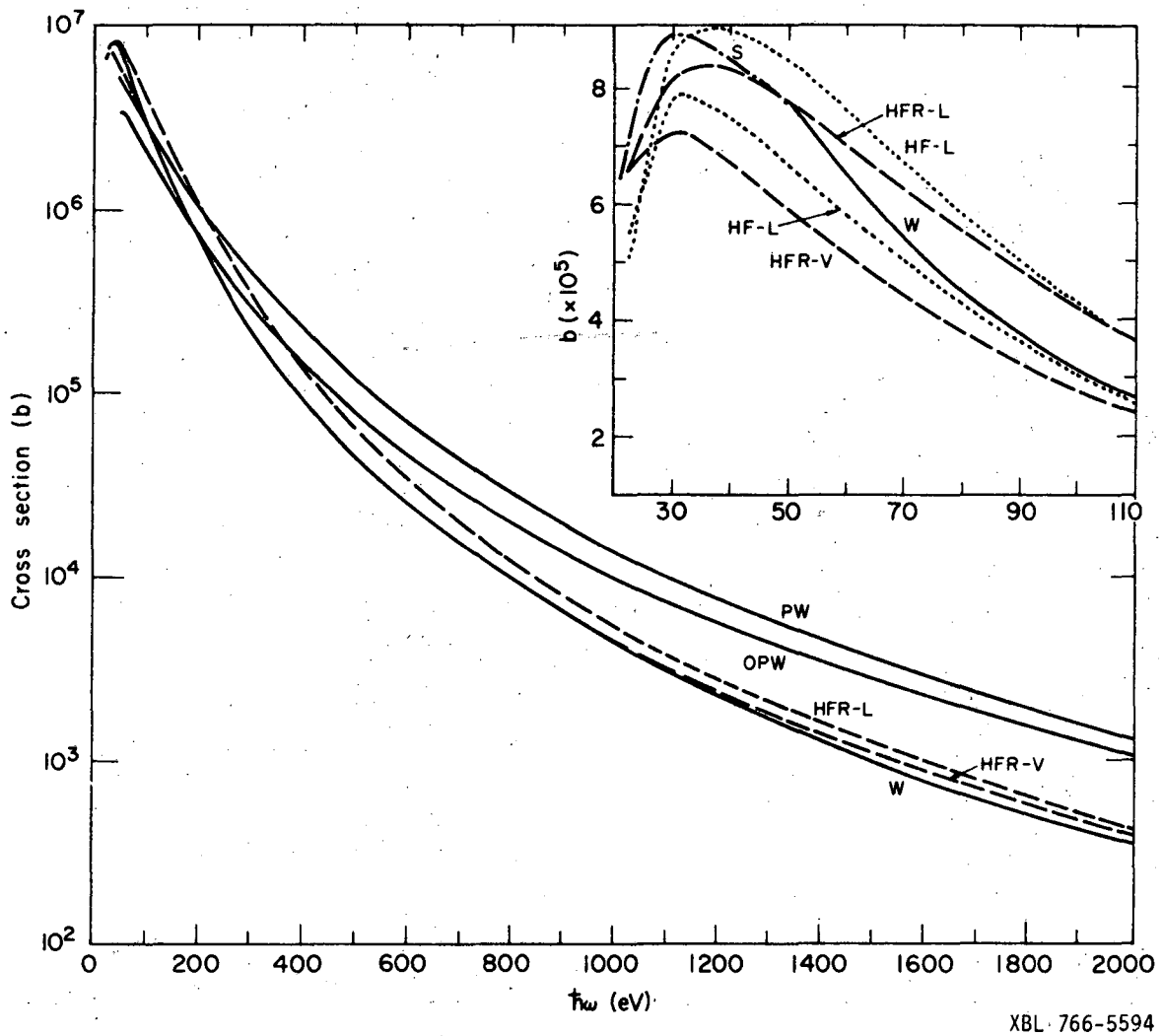
Cross section (b)
10^7
10^6
10^5
10^4
10^3
10^2
0
200
400
600
800
1000
1200
1400
1600
1800
2000
$\hbar\omega$ (eV)
PW
OPW
HFR-L
HFR-V
W
b ($\times 10^5$)
8
6
4
2
30
50
70
90
110
S
HFR-L
HF-L
HF-L
HFR-V
W
XBL 766-5594

Fig. 3

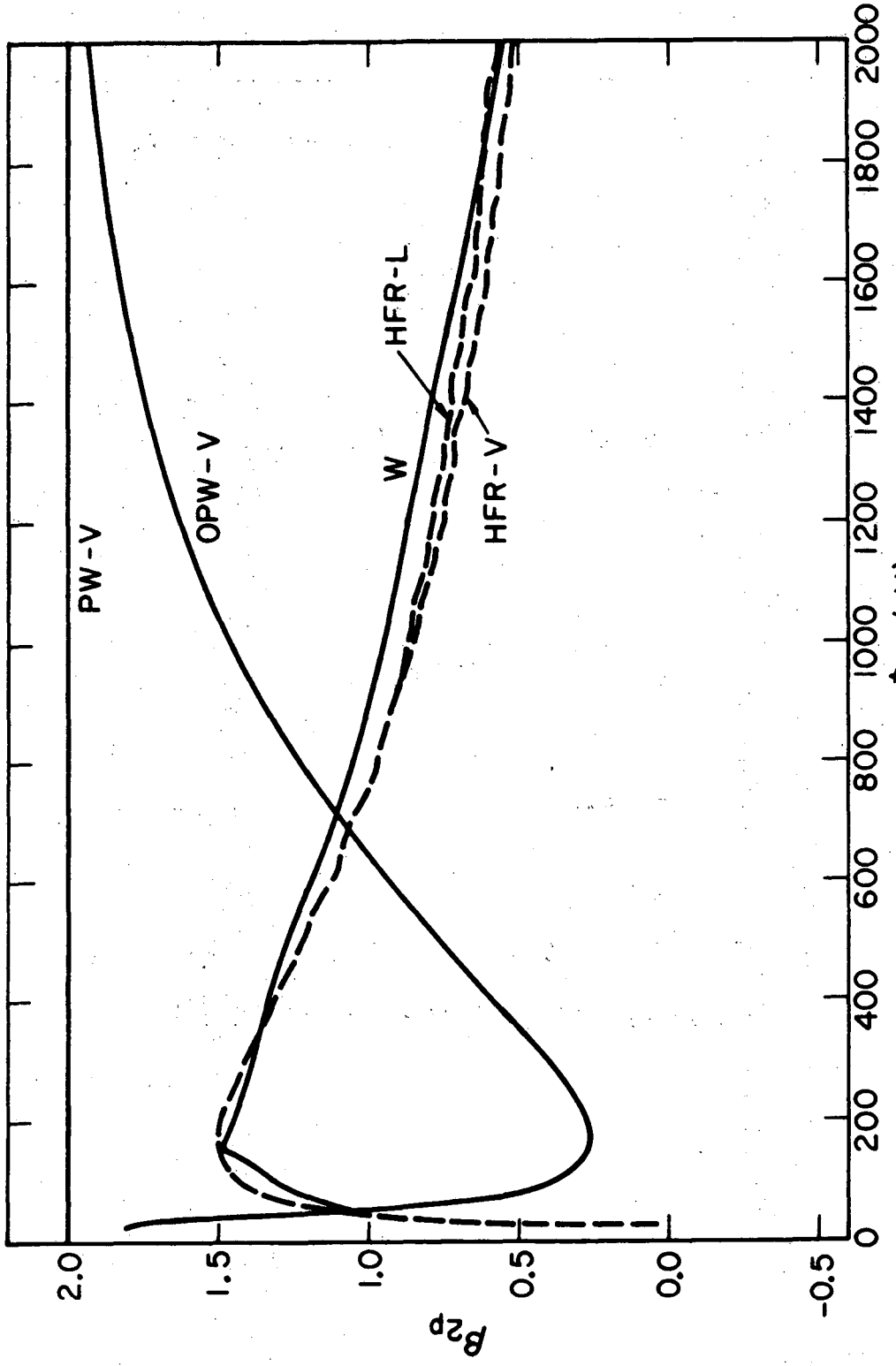

XBL766-5598

Fig. 4

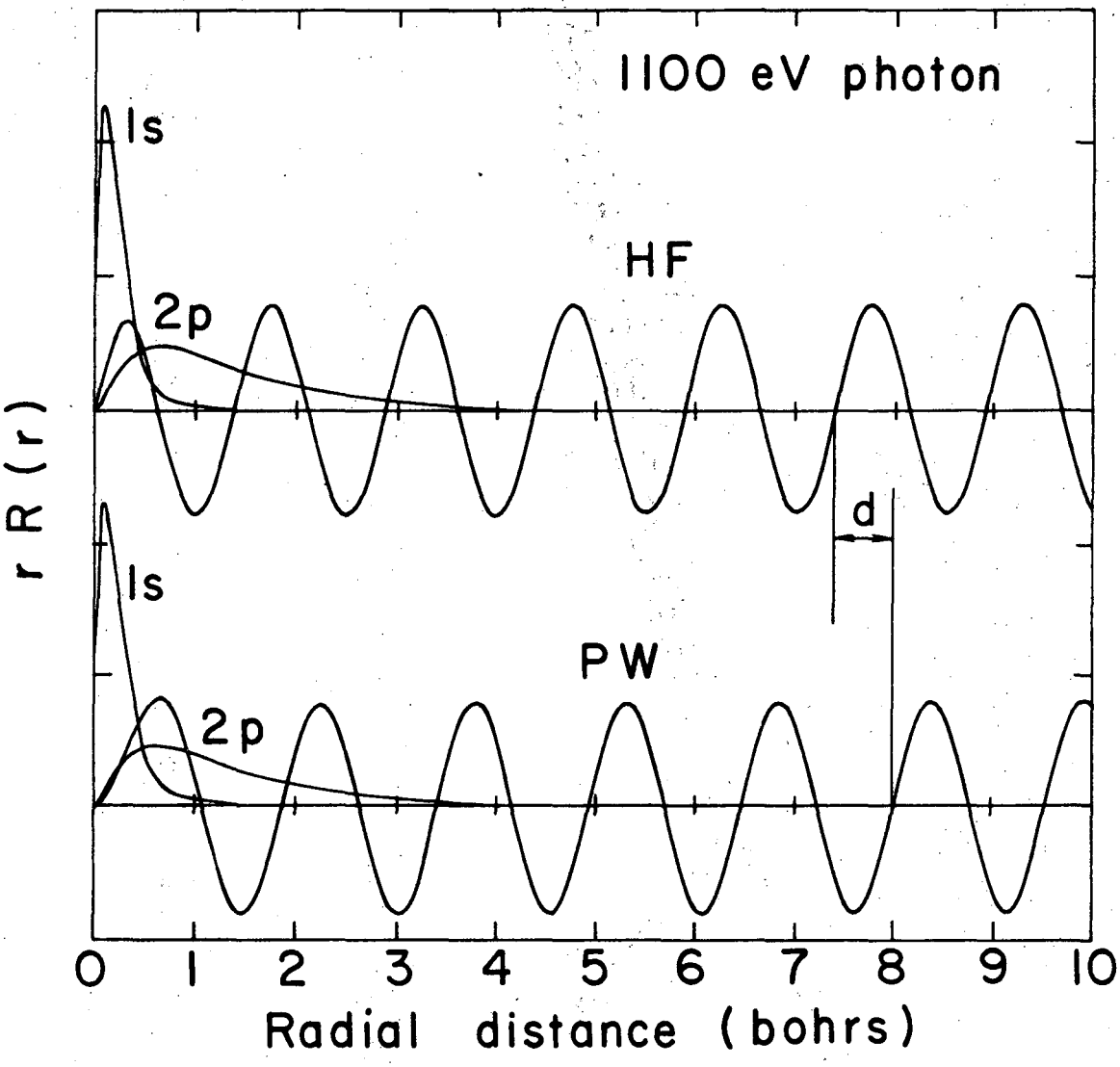

XBL7510-8621

Fig. 5

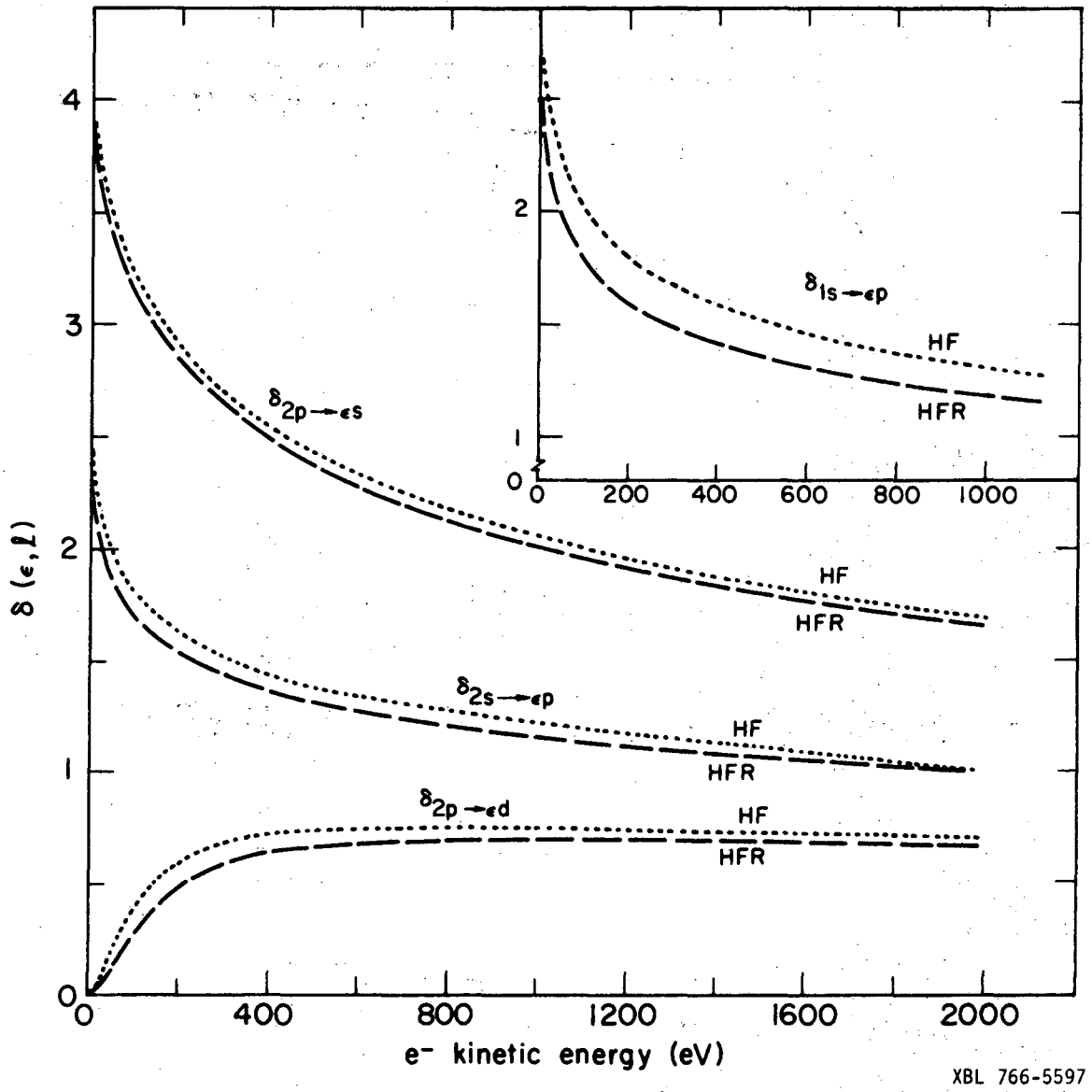

XBL 766-5597

Fig. 6

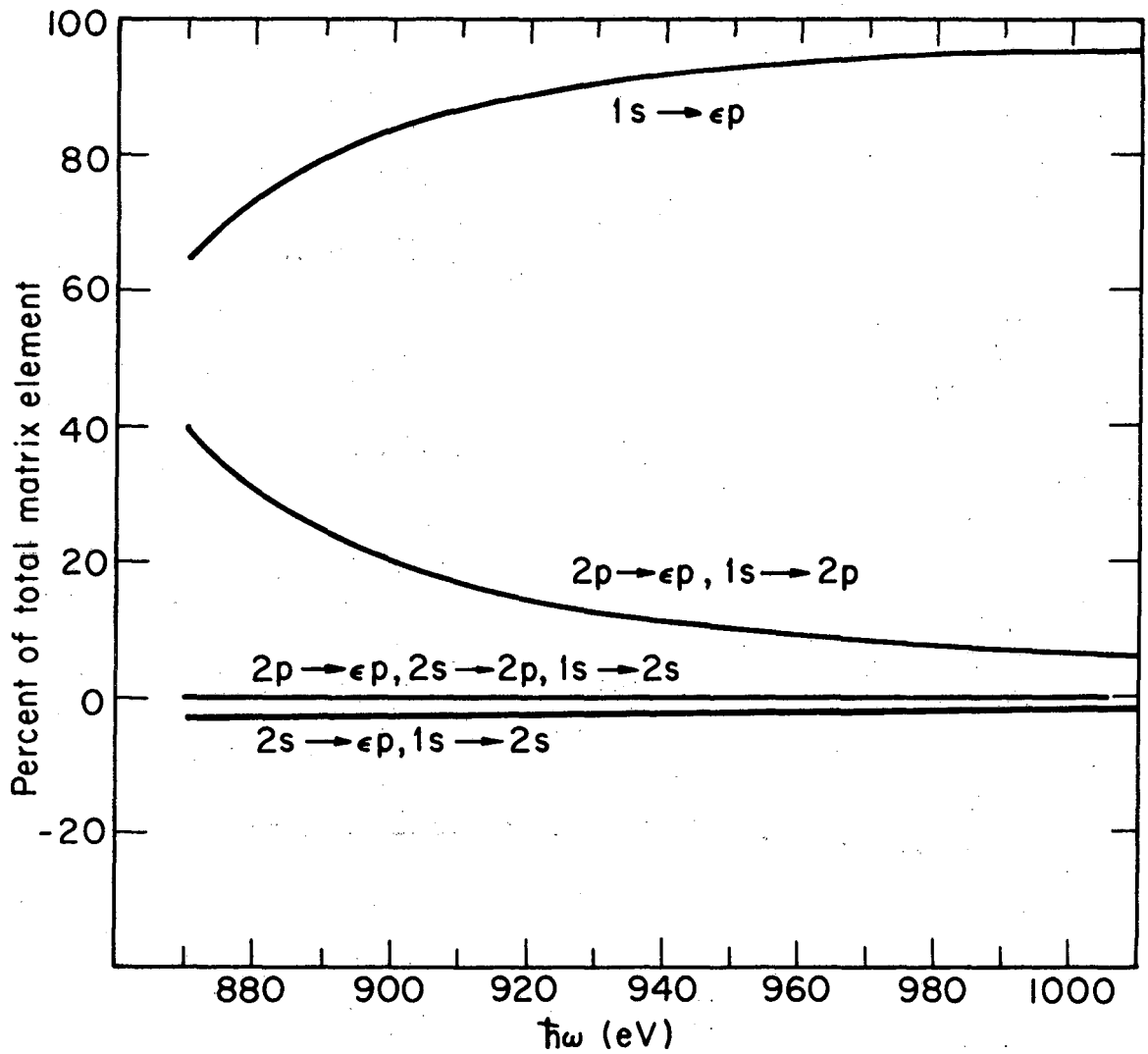

XBL766-5599

Fig. 7

This report was done with support from the United States Energy Research and Development Administration. Any conclusions or opinions expressed in this report represent solely those of the author(s) and not necessarily those of The Regents of the University of California, the Lawrence Berkeley Laboratory or the United States Energy Research and Development Administration.

TECHNICAL INFORMATION DIVISION
LAWRENCE BERKELEY LABORATORY
UNIVERSITY OF CALIFORNIA
BERKELEY, CALIFORNIA 94720